COMPARISON OF BLIND SOURCE SEPARATION ALGORITHMS FOR FMRI USING A NEW MATLAB TOOLBOX: GIFT

Nicolle Correa, Tülay Adalı, and Yi-Ou Li

University of Maryland, Baltimore County
Department of CSEE
Baltimore, MD 21250

Vince D. Calhoun

Olin Neuropsychiatry Research Center
Institute of Living, Hartford, CT 06106
Yale University, New Haven, CT 06520

ABSTRACT

We study the performance of five blind source separation (BSS) algorithms when applied to analysis of functional magnetic resonance imaging (fMRI) data. We introduce a Matlab-based toolbox, the group ICA of fMRI toolbox (GIFT), which enables analysis of groups of subjects using BSS algorithms, in particular those based on independent component analysis (ICA). We use the visualization and computational tools included in GIFT to quantitatively analyze the performance of different BSS algorithms for fMRI analysis and discuss the results.

1. INTRODUCTION

Blind source separation, in particular independent component analysis, has been successfully applied to functional Magnetic Resonance Imaging data [14]. Majority of applications of ICA to fMRI use the Infomax [1] algorithm, and few comparative studies [8, 16] included the use of FastICA algorithm [11] and the second-order Molgedey-Schuster algorithm [15]. In this paper, we study the performances of a number of BSS/ICA algorithms when applied to fMRI data in the user-friendly environment of a Matlab-based toolbox, GIFT [12].

Group analysis of fMRI is important to study specific clinical and experimental conditions within or between groups of subjects. Unlike the general linear model (GLM) and other univariate methods that can easily be generalized to group analysis, subjects as processed by ICA do not share common regressors thus making it difficult to draw group inferences. GIFT implements group study of fMRI data using the group ICA method introduced in [3]. The toolbox includes options for data preprocessing, analysis using BSS/ICA, and visualization tools that can qualitatively evaluate separation results within a user friendly graphical interface. A number of algorithms have been implemented in GIFT (using the versions of these algorithms available online and from ICALAB [6]) and those we have used for the comparative study in this paper are: Infomax [1], FastICA [11], joint approximate diagonalization of eigenmatrices (JADE) [5], simultaneous blind extraction using cumulants (SIMBEC) [7], and algorithm for multiple unknown signal extraction (AMUSE) [18] using delay estimation [9]. In this paper, we use both simulated fMRI-like data and actual fMRI data for the task, address the properties of the expected sources (components) in fMRI data and discuss how these algorithms behave for the separation of these and what the tradeoffs are.

Research supported in part by the NIH award, 1 R01 EB 000840-02.

2. ICA OF FMRI DATA

FMRI is a technique to measure brain activity by recording changes in the magnetic properties of oxygenated and de-oxygenated blood due to neuronal activation. The fMRI data is acquired by recording these blood oxygen level dependent changes by repeatedly scanning brain slices while applying functional stimuli.

Localization and connectionism [17] are said to be the two main characteristics of the brain. This implies that different areas of the brain are responsible for different functions and there is either highly localized or functionally distributed activity in spatially independent areas. An additional assumption of the brain function model is that its hemodynamic response function causes mixing of the neuronal activity in adjacent or overlapping sources resulting in a linear mixture of activity in each slice. ICA algorithms are applied to fMRI to separate the mixture into either spatially independent brain maps and their activation time courses (spatial ICA) or temporally independent time courses and the corresponding spatial maps (temporal ICA).

In this paper, we focus on the spatial ICA model which aims to factorize the mixture $\mathbf{X}$ into independent brain maps, each with a corresponding time course of activation as $\mathbf{X} = \mathbf{AS}$. The dimensions of matrix $\mathbf{A}$ are determined by the number of time points and the number of sources; each element a_{ij} represents the level of activation of the j^{th} source at the i^{th} time point. The dimensions of source matrix $\mathbf{S}$ are determined by the number of sources and the number of voxels; each element s_{jk} determines the contribution of the j^{th} source to the k^{th} voxel. Hence, not only the sources but also the time courses of the separated components are estimated. Obviously, this is not the case for GLM and other similar regression-type methods, where a temporal model is convolved with an estimate of the hemodynamic function and then used as the time course. Thus ICA analysis could reveal characteristics of the brain function that cannot be modelled due to lack of prior information, making ICA a popular tool for fMRI analysis.

3. TOOLBOX

3.1. GIFT

GIFT is a MATLAB-based ICA/BSS tool that includes a number of analysis and visualization tools in a user friendly graphical interface. In this paper, we use the analysis tools to perform ICA on fMRI and fMRI-like data and use the visualization tools to draw inferences on the results obtained.

The analysis tools consist of three processing steps: 1) Pre-ICA: The processing of high-dimensional fMRI data poses com-

putational difficulties and calls for data reduction prior to source separation by the chosen algorithm. In GIFT, principal component analysis (PCA) is used to whiten the data by performing an orthogonal transformation and to reduce the number of principal components present in the mixture. 2) ICA/BSS: The reduced data is then concatenated together and processed by a selected separation algorithm. Thus instead of performing ICA on each subject and then ordering components for comparison across subjects, this method combines the reduced data from different subjects before performing ICA. 3) Post-ICA: The estimated components are representative of the group of subjects and steps such as back-reconstruction are included to obtain individual subject components.

The visualization tools include methods to correlate the obtained spatial maps and time courses to corresponding *a priori* experiment based paradigms, which are useful to categorize components into task-related, transiently task-related, physiology-related, and motion-related components. A brief discussion on the statistical properties of these components is included in the next section. In this paper, while evaluating the results for an fMRI experiment, we use the temporal multiple regression sorting option in GIFT to find the two most task-related components.

3.2. Algorithms Tested

A number of ICA/BSS algorithms have been included in GIFT. Here we briefly introduce the five algorithms whose performance we compare in this paper.

Infomax [1] maximizes the information transfer from the input to the output of a network using a non-linear function. We use the extended Infomax algorithm [13] to improve separation of sources from a mixture containing both super-gaussian (sources of interest) and sub-gaussian sources (artifacts) with natural gradient updates.

FastICA [11] maximizes the higher order statistics or the negentropy of the output to maximize the non-gaussianity of the estimated sources using fixed-point iterations. We use the symmetric FastICA approach with non-linearities *tanh*, *gauss*, and *pow3* [10] to study its separation behavior.

JADE [5] uses the Jacobi technique, to perform joint approximate diagonalization on fourth order cumulant matrices to achieve spatial independence among sources. We use the Matlab optimized version of JADE with a reduced number of eigenmatrices [6].

SIMBEC [7] uses natural gradient ascent in a Stiefel manifold to simultaneously extract sources using a contrast function based on higher order cumulants with a learning rate that provides fast convergence.

AMUSE [18] is a second order BSS algorithm that utilizes the structure within the data to obtain uncorrelated components. It performs singular value decomposition on the shifted cross-variance matrix and the shift is chosen such that the autocorrelations of sources at that shift are non-zero and as different from each other as possible. To choose the shift, we use the method introduced in [9] for the Molgedey-Schuster [15] algorithm, which is based on the same principle as AMUSE.

Codes used in GIFT for SIMBEC and AMUSE are those implemented in ICALAB [6], which is a MATLAB-based toolbox for BSS. The codes for the other three algorithms are available online.

4. PROPERTIES OF FMRI SOURCES

We give a brief overview of fMRI source properties as these properties help in evaluating the separation behavior of the algorithms.

FMRI sources can be classified into sources of interest and artifacts [2]. The sources of interest include task-related, transiently task-related, and function-related sources. These sources are typically super-gaussian in nature because of localization of brain functionality. A task-related source (component) closely matches the experimental paradigm. A transiently task-related time course, on the other hand, is similar to a task-related time course but with an activation that may be pronounced during the beginning of each task cycle and may fade out or change as time progresses. Functional sources are those activated areas which are related to a particular functional area of the brain and are those for which the time course exhibits no particular pattern.

The class of uninteresting sources or artifacts include motion related sources due to head movement, respiration, and cardiac pulsation. The time course for head motion may vary slowly with sudden transient fluctuations. The time courses of the respiratory and cardiac pulsation components may appear to be random fluctuations. Scanner drift is another artifact and is characterized by a slowly rising time course. The activation areas due to artifacts are usually spread over a wider area and are sub-gaussian in nature.

The simulated fMRI-like data given in the next section includes a representative set from both types of sources, those that are of interest and those that are due to artifacts.

5. EXPERIMENT

5.1. Simulated fMRI-like data

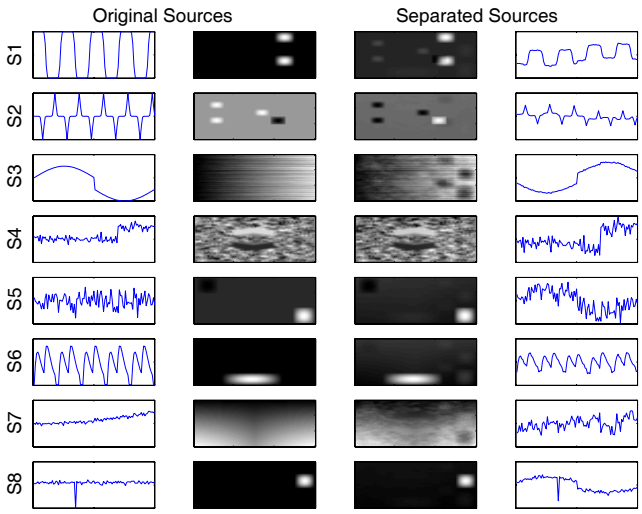

Fig. 1. Original and estimated sources using Infomax for Set-2

Using the basic knowledge of the statistical characteristics of the underlying sources as explained in Section 4, we simulate fMRI-like source images and mix them with the selected time courses to obtain a set of mixtures. We present results with two data sets. Set-1 (first five in Fig. 1) consists of three highly super-gaussian sources, a gaussian source and a sub-gaussian source and the time courses represent sources that are task-related (S1), transiently task-related (S2) and artifact-related (S3, S4, and S5). Set-2 given in Fig. 1, consists of the same five sources with an additional sub-gaussian source (S7) and two more super-gaussian sources

Algorithm	Spatial Correlation Coefficients					Convergence Time (seconds)	
	S1 $\kappa = 23.27$	S2 $\kappa = 25.80$	S3 $\kappa = -1.15$	S4 $\kappa = 0.43$	S5 $\kappa = 23.64$	Set-1	Set-2
FastICA gauss	0.95±0.07	0.95±0.12	0.86±0.12	0.91±0.13	0.97±0.07	0.6±0.36	20.35±2
FastICA tanh	0.98±0	1±0	0.83±0.13	0.87±0.14	1±0	0.43±0.28	20.35±6.75
FastICA pow3	0.97±0	1±0	0.78±0.13	0.81±0.14	0.99±0	0.65±0.32	26.36±6.61
Infomax	0.96±0	0.99±0	0.95±0.01	0.97±0.01	0.98±0	10.95±1.28	13.29±1.79
JADE	0.93	1	0.9	0.94	0.99	0.05	0.19
SIMBEC	0.98	0.93	0.98	0.71	0.6	0.25	0.28
AMUSE	0.92±0.02	0.77±0.04	1±0	0.75±0.08	0.92±0	0.89±0.24	1.11±0.64

Table 1. Correlation of original and estimated sources for Set-1 and convergence time for both sets (κ denotes the kurtosis)

with transiently task-related and random (artifact) time courses (S6 and S8 respectively). Each simulated source is a 60×60 image with a 100-point time course. The image data is reshaped into vectors by concatenating columns of the image matrix. The source matrix $\mathbf{S}$ is multiplied by the time course matrix $\mathbf{A}$ to obtain a mixture that simulates 100 scans of a single slice.

Twenty runs are performed for FastICA and Infomax to take into account random initial conditions. Due to the dependence on the choice of the spatial shift we perform twenty runs on AMUSE and change the initial shift value for each run. JADE and SIMBEC are deterministic algorithms and hence the results are given for a single run. To quantify performance, the averages are calculated over different runs for the temporal and spatial correlation of the estimated and the original sources. Spatial correlation coefficients for Set-1 and time taken by each algorithm for both sets are given in Table 1. Due to space limitations, the numerical values for the temporal correlation results of Set-1 and the results for Set-2 are not given. However, we present a brief overview of these results.

All five algorithms were able to achieve some separation of the sources, with significant performance differences especially for the second data set. The performances of Infomax and JADE were comparable for most cases, with Infomax yielding slightly better overall performance.

FastICA yields high spatial correlation values for super-gaussian sources and slightly lower values for the other sources. For Set-1, FastICA with the *gauss* non-linearity provides better performance compared to the other two non-linearities for the gaussian and sub-gaussian sources. However, for Set-2 all three non-linearities result in very similar performance. Overall, the general performance of FastICA using *tanh* is better than the results obtained using the other two non-linearities.

SIMBEC performs well for the sources of interest in Set-1, e.g., for the task-related source S1 and transiently task-related source S2 and also for the sub-gaussian source S3. However, the results for Set-2 using SIMBEC, were poor except for the sub-gaussian sources. For Set-1, AMUSE fails to completely separate sources S2 and S4 but performs well for the other sources while for Set-2, it almost completely fails.

Temporal correlation of the time courses in Set-1 is high for all the algorithms except AMUSE which has trouble estimating the transiently task-related time course. SIMBEC fails to estimate some of the time courses, it results in a null time course for sources S4 and S6. All the algorithms were unable to completely identify the random time course of source S5. The temporal correlation coefficients for Set-2 are in general lower than those for Set-1.

In terms of convergence, Infomax has been the slowest for Set-1. For Set-2, FastICA exhibited the slowest convergence due to stability problems and we used the stabilized version of FastICA to achieve convergence for this set. In our runs with other simulated data, the convergence problems seemed to be pronounced when more than one sub-gaussian source was present in the mixture. In the stabilized version, the step size is halved if convergence is not reached after half the maximum number of iterations and also when the algorithm is stuck between two points.

5.2. FMRI data

Algorithm	Temporal MCCs		Time (sec)
FastICA gauss	0.75±0.01	0.65±0.03	2±1.07
FastICA tanh	0.75±0.01	0.66±0.01	1.15±1.41
FastICA pow3	0.78±0.03	0.68±0.02	14.12±8.89
Infomax	0.77±0	0.65±0	0.9±0.12
JADE	0.73	0.65	1.09
SIMBEC	0.7	0.63 & $0.51^{(*)}$	0.17
AMUSE	0.84±0.01	0.46±0.08	0.72±0.55

Table 2. Temporal multiple correlation coefficients (MCCs) for the two most task-related components and convergence time

We perform group ICA on fMRI data from three subjects performing a visuomotor task [4]. A single slice passing through the visual cortex is analyzed for each subject. Using PCA, each subject's data is first reduced to twenty components. After concatenating the reduced components from the three subjects, we perform a second reduction step and reduce the number of components to eight, as discussed in [3] . The separation results thus will be representative of the entire group and not the individual subjects. Using GIFT, we scale the results to Z-scores and set the threshold value to $Z = 1.5$. The separated components are sorted using temporal multiple regression by comparing the estimated time courses to the model paradigm to find the two most task-related components. In this case, for the non-deterministic algorithms, ten runs are performed and the stabilized version of FastICA is used since the algorithm had convergence problems especially while using the *pow3* non-linearity.

The results of the ICA algorithms for fMRI data reveal task-related, transiently task-related, and motion-related sources among the separated components. MCC values of the two most task-related components are listed in Table 2. We observe that all the algorithms do well, with FastICA using the *pow3* non-linearity performing slightly better in terms of closeness to the model time course. Notice that even though the first MCC value is very high for AMUSE, the second one is low. Two MCC values $^{(*)}$ are listed for the second task-related component for SIMBEC. These issues with AMUSE and SIMBEC are discussed later in this section.

Infomax, FastICA, and JADE successfully find task-related components in the left and right visual hemifields. In Fig. 2. we display the component from the results of each algorithm which

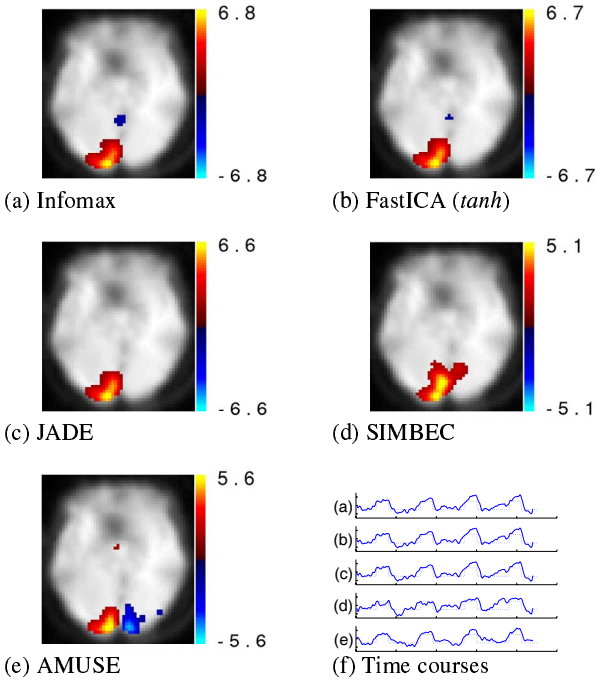

Fig. 2. FMRI single slice results (left visual cortex)

contains the left visual cortex activation. Among the components not displayed some interesting differences are worth noting. We observed that the spatial extent of the task-related component in the right visual area is slightly larger for Infomax and FastICA estimations as compared to JADE. For the transiently task-related component the spatial extent is slightly higher in FastICA and JADE compared to Infomax. The performance of FastICA is similar for all three non-linearities, with slightly higher correlation values for *pow3*. In Fig. 2, we see that the Z-scores for Infomax are higher than the other algorithms for the task-related source, indicating that Infomax achieves a higher contrast to noise ratio.

SIMBEC identifies the two task-related sources in the right and left hemifields, however it splits the left hemifield task-related source into two components, one of which is showed in Fig. 2 (d). AMUSE also finds the two task-related sources but places both in the same component (Fig. 2 (e)) as seen by the high MCC value of the most task-related component and low value of the second most task-related component. This may be because the left and right activations for the task-related source have similar spectra.

6. DISCUSSION

We have compared the performance of the five algorithms for performing BSS/ICA of fMRI data. Based on our results, Infomax emerged as a reliable choice for the task, followed by JADE as a close second. FastICA performed reliably for most cases as well whereas the performance of SIMBEC and AMUSE did not prove to be robust, different combination of sources and their numbers seemed to affect the performance significantly. SIMBEC, however, may prove to be useful to identify the sub-Gaussian sources, i.e., artifacts in fMRI data as its performance for these sources has been consistently very good. The performance of AMUSE is highly dependent on the differentiability of the spectra of the sources for a given delay and its performance suffers a great deal when the condition is not met. In our simulations, we observed that the condition is limiting for fMRI data especially when the number of sources increase. While our simulations with actual fMRI data has been useful in highlighting some limitations of certain algorithms, it should be emphasized that the performance evaluation in this case is limited since no ground truth is available. Evaluation by using correlation with a time series does not take into account the fact that ICA is able to bring out characteristics of the brain function that are not completely predictable.

Acknowledgment: Authors would like to thank Dr. Cichocki for providing part of the codes and for his valuable input.

7. REFERENCES

[1] A. J. Bell and T. J. Sejnowski, "An information maximisation approach to blind separation and blind deconvolution," *Neural Comput.*, vol. 7, pp. 1129–1159, 1995.

[2] V. D. Calhoun, T. Adalı, L. K. Hansen, J. Larsen and J. J. Pekar, "ICA of functional MRI data: an overview," *Proc. Int. Symp. Indep. Comp. Analysis (ICA 2003)*, Nara, Japan.

[3] V. D. Calhoun, T. Adalı, G. D. Pearlson and J. J. Pekar, "A method for making group inferences from functional MRI data using independent component analysis," *Human Brain Mapping*, vol. 14, pp 140–151, 2001.

[4] V. D. Calhoun, T. Adalı, J. J. Pekar and G. D. Pearlson , "Latency (in) sensitive ICA: group independent component analysis of fMRI data in the temporal frequency domain," *NeuroImage*, vol. 20, no. 3, pp. 1661–1669, 2003.

[5] J. F. Cardoso and A. Souloumiac, "Blind beamforming for non gaussian signals," *IEE-Proc-F*, vol. 140, no. 6, pp. 362–370, 1993.

[6] A. Cichocki, S. Amari, K. Siwek, T. Tanaka et al., "ICALAB Toolboxes," http://www.bsp.brain.riken.jp/ICALAB.

[7] S. Cruces, A. Cichocki and S. Amari, "Criteria for the simultaneous blind extraction of arbitrary groups of sources," *Int. Conf. Indep. Comp. Analysis and Blind Sig. Sep.*, San Diego, California, USA, 2001.

[8] F. Esposito, *et al.*, "Spatial independent component analysis of functional MRI time-series: to what extent do results depend on the algorithm used?," *Human Brain Mapping*, vol. 16, pp 146–157, 2002.

[9] L. K. Hansen, J. Larsen and T. Kolenda,"Blind detection of independent dynamic components," *IEEE Proc. ICA 2001*, San Diego, USA. pp. 540–545.

[10] A. Hyvärinen, "Fast and robust fixed-point algorithms for independent component analysis," *Neural Networks*, vol. 10, pp. 626–634, 1999.

[11] A. Hyvärinen and E. Oja, "A fast fixed-point algorithm for independent component analysis," *Neural Comput.*, vol. 9, no. 7, pp. 1483–1492, 1997.

[12] GIFT, `http://icatb.sourceforge.net`.

[13] T. W. Lee, M. Girolami, and T.J. Sejnowski, "Independent component analysis using an extended Infomax algorithm for mixed sub-Gaussian and super-Gaussian sources, *Neural Computation*, vol. 11, no. 2, pp. 417–441, 1999.

[14] M. J. Mckeown, *et al.* "Analysis of fMRI by blind separation into independent spatial components," *Human Brain Mapping*, vol. 6, no. 3, pp 160–188, 1998.

[15] L. Molgedey and H. Schuster, "Separation of independent signals using time-delayed correlations," *Physical Review Letters*, vol. 723, pp. 3634-37, 1994.

[16] K. S. Petersen, L. K. Hansen, T. Kolenda, E. Rostrup and S. C. Strother, "On the independent components of functional neuroimages," *Proc. of ICA-2000*, Finland.

[17] C. G. Phillips, S. Zeki and H. B. Barlow, "Localization of function in the cerebral cortex. Past, present and future," *Brain*, vol. 107, pp. 327–361, 1984.

[18] L. Tong, V. C. Soon, Y. F. Huang and R. Liu, "Indeterminacy and identifiability of blind identification," *IEEE Trans. Circuits Sys.*, vol. 38, pp. 499–509, 1991.